Field-induced quasiparticle excitations in novel type II superconductors



2004 J. Phys.: Condens. Matter 16 S4421

(http://iopscience.iop.org/0953-8984/16/40/002)

INSTITUTE OF PHYSICS PUBLISHING JOURNAL OF PHYSICS: CONDENSED MATTER

J. Phys.: Condens. Matter **16** (2004) S4421–S4438 PII: S0953-8984(04)84288-7

# Field-induced quasiparticle excitations in novel type II superconductors

**R Kadono**

Institute for Materials Structure Science, High Energy Accelerator Research Organization (KEK), Tsukuba, Ibaraki 305-0801, Japan
and
School of Mathematical and Physical Science, The Graduate University for Advanced Studies, Tsukuba, Ibaraki 305-0801, Japan

Received 15 March 2004
Published 24 September 2004
Online at stacks.iop.org/JPhysCM/16/S4421
doi:10.1088/0953-8984/16/40/002

**Abstract**

We show that the field dependence of the magnetic penetration depth ($\lambda$), for which muon spin rotation ($\mu$SR) is an excellent microscopic probe, provides useful information on the degree of anisotropy of the superconducting order parameter. In type II superconductors associated with anisotropic order parameters, $\lambda$ is sensitive to the quasiparticle excitation induced by the Doppler shift due to a supercurrent around magnetic vortices. The presence of such low energy excitations manifests itself in the non-zero slope of $\lambda$ against an external magnetic field. We review recent results on the field dependence of $\lambda$ obtained from the application of $\mu$SR to novel superconductors that exhibit unconventional characters associated with the anisotropic order parameter.

## 1. Introduction

One of the greatest impacts of the discovery of high $T_c$ cuprate superconductors is renewed interest in the exotic mechanisms of superconductivity, and a boosted search for their model systems, which has led to a soaring number of novel materials identified as superconductors [1]. They include varieties of transition metal oxides, borides, borocarbides, and other intermetallic compounds with rare-earth elements. The list can be readily extended by including those based on organic materials, and is still growing in length. Compared with classical simple metals or binary compound superconductors, they have a common distinctive feature that the pairing correlation is potentially highly anisotropic due to a strong electronic correlation (Coulomb repulsion) and/or a considerably two-dimensional nature of the Fermi surface, which is also shared by cuprate superconductors.

It is well established that any metallic system can fall into a superconducting state when there is an effective interaction that is attractive between the conduction electrons (pair correlation). In this situation, electrons tend to form a bound (pairing) state between those with

  

opposite momenta (**k** and $-$**k**), so the phase of the pairing wavefunction may become absolute zero [2]. This instability towards the formation of electronic bound states without a barrier is an intrinsic characteristic of the Fermi surface, irrespective of the microscopic mechanism of the attractive interaction. When the pair correlation is mediated by the electron–phonon interaction, as in ordinary cubic metals, the pair correlation has the least dependence on **k** (the relative orbital angular momentum $L = 0$), and thereby the structure of the superconducting order parameter $\Delta(\mathbf{k})$ is isotropic over the entire Fermi surface. Because of the mandatory requirement of Fermi statistics that the electronic wavefunction must be antisymmetric, the remaining freedom of the spin state in the pairing function is set to being a singlet ($S = 0$). This pair correlation, having s-wave and spin singlet symmetry, is conventionally called the 'BCS mechanism'; in its narrower sense, the electron–phonon interaction is presumed to be the primary origin of the attractive interaction [3].

Historically, the first sign of non-BCS-type pairing was found in the superfluidity of liquid $^3$He [4, 5], where the neutral $^3$He atoms (which have a nuclear spin of 1/2 and thereby obey Fermi statistics) play the role of electrons in superconductivity. It is known that liquid $^3$He can be regarded as being a Fermi liquid (i.e., having a well-defined Fermi surface) below $\sim 10^2$ mK, and that it becomes a superfluid below a few mK, where it can flow through narrow channels without friction (superfluidity). However, there is a major difference between the nature of the pairing between $^3$He atoms and that of the BCS type. The $^3$He atom has a hard core having a repulsive interaction with a relatively large radius, which makes it difficult to pair in a state with zero angular momentum. Thus, many theories have predicted that $^3$He atoms may pair in a p-wave ($L = 1$) or d-wave ($L = 2$) state, where they can keep themselves apart while the pairing interaction is at work [6, 7]. Later, experiments confirmed that they were indeed in a p-wave state. This also meant that the spin part of the pairing wavefunction (order parameter) must be in a triplet state ($S = 1$), leading to a variety of possibilities for the total state of the pairing wavefunction ($\propto \Delta(\mathbf{k})$) for breaking symmetry. It is now established that there are at least three different phases in the superfluidity of liquid $^3$He that all have different order parameters.

It is readily predicted that a situation similar to that in liquid $^3$He can be realized when a short range repulsive electronic correlation is not negligible in metallic superconductivity. As has been established during the past decade, high $T_c$ cuprates are among the first such examples in which electrons pair in a state other than an s-wave one due to a strong on-site repulsive correlation. The Cooper pairs in cuprates prefer a d-wave state because of the tetragonal structure of the two-dimensional $CuO_2$ lattice and the associated symmetry of the Fermi surface. More specifically, the pairing is a $d_{x^2-y^2}$ wave and the order parameter is described by a gap function,

$$\Delta(\mathbf{k}) = \Delta_0(\cos k_x - \cos k_y) \simeq \Delta_0(k_y^2 - k_x^2), \tag{1}$$

where $\Delta_0$ is the maximum value of the anisotropic gap; the energy gap vanishes along the lines $k_x = \pm k_y$, which are called *line nodes*. It also happens that the electronic correlation in cuprates is antiferromagnetic, as is naturally expected for doped Mott insulators, which makes it favourable for forming spin singlet pairs. The latter points to a magnetic origin as a pairing mechanism, irrespective of the true nature of the ground state which is still under debate. Thus, the structure of the superconducting order parameter reflects important characteristics of the electronic correlation.

In this paper, we review our recent studies on the structure of the superconducting order parameter in novel type II superconductors by means of muon spin rotation/relaxation ($\mu$SR). It is well known that a magnetic field can penetrate type II superconductors as a bundle of quantum flux lines (magnetic vortices) [8], where the spatial field distribution, $B(\mathbf{r})$, becomes

inhomogeneous due to gradual change in the supercurrent flow around the vortices. The degree of inhomogeneity, which is primarily determined by the magnetic penetration depth ($\lambda$), a magnetic cut-off parameter ($\xi_v$, which is proportional to the Ginzburg–Landau (GL) coherence length $\xi_{GL}$), and the spacing of vortices ($a$) can be measured directly via $\mu$SR as a spin–spin relaxation ($1/T_2$). By applying a refined analysis technique, one can reconstruct $B(\mathbf{r})$ more accurately so that both $\lambda$ and $\xi_v$ may be deduced separately [9]. Among various experimental techniques applied to a similar end, the $\mu$SR technique is unique in many respects. Namely, it is a microscopic technique that can be applied to virtually any superconductors having a reasonable magnetic penetration depth ($\lambda \leqslant 5000$ Å). Also, because of the purely magnetic nature of a spin 1/2 probe, the interpretation of the $\mu$SR spectra is free from any complication due to additional interactions from higher multipoles often found in nuclear magnetic resonance (NMR). The $\mu$SR technique is sensitive to the bulk property, and is thus free from effects specific to the surface, while they often present problems for scanning tunnelling spectroscopy (STS) and angle-resolved photoemission spectroscopy (ARPES).

In the following, we demonstrate that the temperature/field dependence of $\lambda$ is strongly affected by the anisotropy of the order parameter. In particular, $\lambda$ is enhanced by an external field due to the Doppler shift of quasiparticles in the gap nodes [10], which leads to almost a linear increase of $\lambda$ with increasing field. This feature is regarded as an unambiguous sign of the presence of nodes in the energy gap or that of a small energy gap in the multi-gap order parameter. We show several examples of field-dependent $\lambda$, some of which are indeed identified to have anisotropic (or multi-gap) order parameters by other experimental techniques. A more comprehensive review of a similar study can be found elsewhere [9].

## 2. The internal magnetic field distribution in the mixed state

### *2.1. The microscopic model*

In penetration depth measurements, it is common to assume a geometrical condition wherein muons are implanted into a specimen with the initial spin polarization perpendicular to the external field, $\mathbf{H} = (0, 0, H)$. Then, since muons stop randomly along the length scale of the flux line lattice (FLL), the time evolution of complex muon polarization, $\hat{P}(t)$, provides a random sampling of the internal field distribution, $\mathbf{B}(\mathbf{r}) = (0, 0, B(\mathbf{r}))$:

$$\hat{P}(t) \equiv P_x(t) + \mathrm{i}P_y(t) = \exp(-\sigma_b^2 t^2) \int_{-\infty}^{\infty} n(B) \exp(\mathrm{i}\gamma_\mu B t + \phi)\, \mathrm{d}B, \tag{2}$$

$$n(B) = \langle \delta(B - B(\mathbf{r})) \rangle_{\mathbf{r}}, \tag{3}$$

where $P_{x,y}(t)$ is proportional to the time-dependent $\mu^+$–$e^+$ decay asymmetry, $A_{x,y}(t)$, deduced from a corresponding set of positron counters, $n(B)$ is the spectral density for the internal field defined as a spatial average ($\langle\,\rangle_{\mathbf{r}}$) of the delta function, $\gamma_\mu$ is the muon gyromagnetic ratio ($=2\pi \times 135.53$ MHz T$^{-1}$), and $\phi$ is the initial phase of muon precession [11, 12]. The additional relaxation ($\sigma_b$) is mainly due to random local fields from nuclear magnetic moments ($\sigma_n \sim 0.1\ \mu s^{-1}$) and the distortion of the flux line lattice due to a random pinning of vortices ($\sigma_p$), which can be approximated by a Gaussian relaxation [11]. These equations indicate that the real amplitude of the Fourier-transformed muon precession signal corresponds to $n(B)$ with an appropriate correction of $\sigma_b$. While $\sigma_n$ can be estimated from the spectrum in the normal state, $\sigma_p$ often needs to be considered as a variable parameter, depending on the temperature and/or external magnetic field.

In modelling the internal field distribution of the vortex state, the simplest approach is to assume that the field distribution is a linear superposition of that for an isolated vortex, as

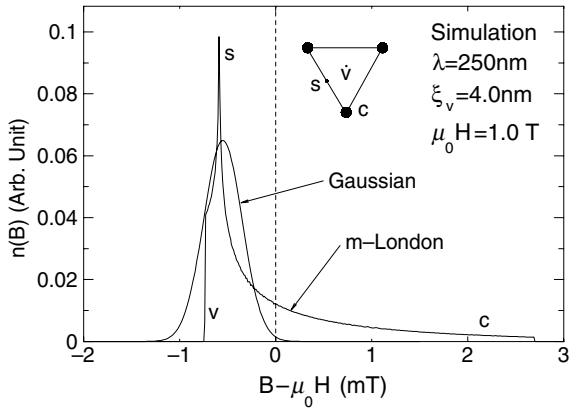


**Figure 1.** A magnetic field distribution $n(B)$ calculated using the modified London model with a triangular flux line lattice. (A Lorentzian cut-off was assumed.) The label 'c' refers to the contribution from vortex cores, 's' to saddles, and 'v' to valleys. The Gaussian distribution is only meant as a guide to the eye.

presumed in the London theory [13]. This is a reasonable assumption as long as the inter-vortex distance is much longer than the GL coherence length ($H \ll H_{c2}$). Then, what we need is to know the field distribution around a single vortex and the structure of the vortex lattice. The latter must be given from other sources of information, such as small angle neutron scattering (SANS) or scanning tunnelling microscopy/spectroscopy (STM/STS). In the London model, $B(\mathbf{r})$ is approximated as the sum of the magnetic inductions from isolated vortices, to yield

$$B(\mathbf{r}) = B_0 \sum_{\mathbf{K}} \frac{\mathrm{e}^{-\mathrm{i}\mathbf{K}\cdot\mathbf{r}}}{1 + K^2\lambda^2} F(K, \xi_\mathrm{v}), \tag{4}$$

where $\mathbf{K}$ are the vortex reciprocal lattice vectors, $B_0$ ($\simeq\mu_0 H$) is the average internal field, $\lambda$ is the London penetration depth, and $F(K, \xi_\mathrm{v})$ is a non-local correction term with $\xi_\mathrm{v}$ being the cut-off parameter for the *magnetic* field distribution; care must be taken not to interpret $\xi_\mathrm{v}$ naively as $\xi_{\mathrm{GL}}$ which is for the spatial variation of the superconducting order parameter. While the Lorentzian cut-off, $F(K, \xi_\mathrm{v}) = \exp(-\sqrt{2}K\xi_\mathrm{v})$, is predicted to be a better approximation for the GL theory at lower fields [14], the Gaussian cut-off, $F(K, \xi_\mathrm{v}) = \exp(-K^2\xi_\mathrm{v}^2/2)$, generally provides satisfactory agreement with the data [15]. Note, however, that the Gaussian cut-off is derived from the GL equations near $H_{c2}$, and thus would not be appropriate at lower fields. A comparison of the analysis on identical data indicates that a Gaussian cut-off yields a significantly larger value for $\lambda$ and a stronger field dependence (about a factor 2) than those obtained with a Lorentzian cut-off [9].

Besides the London model, there are a couple of models for $B(\mathbf{r})$ based on the Ginzburg–Landau theory. Although the GL equations can be solved to yield an approximate analytical solution for the mixed state near $H_{c1}$ or $H_{c2}$, they must be solved numerically for intermediate fields. Fortunately, it is known that the field distribution obtained from exact numerical solutions of the GL equations is in excellent agreement with that from the modified London model at low fields and arbitrary $\kappa$ ($=\lambda/\xi_{\mathrm{GL}}$, the GL parameter) [16].

One of the most important characteristics of $n(B)$ obtained from these models is the site-selective feature of the line shape. As shown in figure 1, the sharp peak due to the van Hove singularity found in the lower field mainly represents the contribution from the saddle points of $B(\mathbf{r})$, the lower field end from the central valleys among vortices, and the high field end from the region near the vortex cores. This quite asymmetric field profile with such a geometrical correspondence allows us to determine $\lambda$ and $\xi_\mathrm{v}$ reliably by comparing the time evolution of the muon spin polarization with that calculated using $n(B)$.

It is often the case that the superconducting properties in non-cubic compounds are strongly anisotropic, leading to a large difference between the magnetic penetration depths for in-plane

and perpendicular directions. More specifically, in uniaxial superconductors with $M_{ab}$ and $M_c$ being the carrier mass for in-plane and perpendicular directions, we have

$$B(\mathbf{r},\theta) = B_0 \sum_{\mathbf{K}} b(\mathbf{K}) \mathrm{e}^{-\mathrm{i}\mathbf{K}\cdot\mathbf{r}} F(K,\xi_\mathrm{v}), \tag{5}$$

$$b(\mathbf{K}) = \frac{1 + K^2 m_{zz}\lambda^2}{(1 + K_x^2 m_{ab}\lambda^2 + K_y^2 m_{xx}\lambda^2)(1 + K^2 m_{zz}\lambda^2) - K^2 K_y^2 m_{xz}^2 \lambda^4}, \tag{6}$$

where $\theta$ is the polar angle of the $c$-axis, $m_{ab} = M_{ab}/\overline{M}$, $m_c = M_c/\overline{M}$ (with $\overline{M} = (M_{ab}^2 M_c)^{1/3}$), and

$$m_{xx} = m_{ab}\cos^2\theta + m_c \sin^2\theta, \tag{7}$$

$$m_{zz} = m_{ab}\sin^2\theta + m_c \cos^2\theta, \tag{8}$$

$$m_{xz} = (m_{ab} - m_c)\sin\theta\cos\theta. \tag{9}$$

Thus, the line shape depends on $\lambda_{ab} = \lambda\sqrt{m_{ab}}$ and $\lambda_c = \lambda\sqrt{m_c}$ in a complex manner [17].

### 2.2. *Gaussian field distribution*

When the quality of $\mu$SR data is good enough to be analysed using the above model, we can obtain $\lambda$ and $\xi_\mathrm{v}$ simultaneously by directly comparing the $\mu$SR time spectrum with that calculated from $B(\mathbf{r})$. Unfortunately, our experience shows that this is not always the case when the sample is not a single crystal, or $\lambda$ happens to be very large, etc, so that the characteristic features of $n(B)$ and the associated time spectra important for such analysis are smeared out. In such a situation, the Gaussian field distribution has been used as a convenient analytical model, where the depolarization rate is presumed to be given by the second moment of the field distribution ($\lambda \gg \xi_\mathrm{v}$),

$$\langle \Delta B^2 \rangle = \langle (B(\mathbf{r}) - \mu_0 H)^2 \rangle_\mathbf{r}, \tag{10}$$

which is reflected as $T_2$ relaxation in the $\mu$SR line shape. The Gaussian distribution of local fields naturally leads to a Gaussian depolarization function,

$$\hat{P}(t) \simeq \exp(-\sigma_\mathrm{b}^2 t^2)\exp(-\sigma^2 t^2/2)\exp(\mathrm{i}\gamma_\mu B_0 t + \phi), \tag{11}$$

$$\sigma = \gamma_\mu \sqrt{\langle \Delta B^2 \rangle}. \tag{12}$$

For the ideal case of a triangular FLL with an isotropic effective carrier mass and a cut-off $K \approx 1.4/\xi_\mathrm{v}$ provided by the numerical solution of the GL theory, $\lambda$ can be deduced from $\sigma$ using the following relation [18, 19, 12]:

$$\sigma(h)\ (\mu\mathrm{s}^{-1}) = 4.83 \times 10^4 (1-h)\lambda^{-2}\ (\mathrm{nm}), \tag{13}$$

where $h = H/H_{c2}$. While the above form is valid for $h < 0.25$ or $h > 0.7$, a more useful approximation valid for an arbitrary field is [12]

$$\sigma(h)\ (\mu\mathrm{s}^{-1}) = 4.83 \times 10^4 (1-h)[1 + 3.9(1-h)^2]^{1/2}\lambda^{-2}\ (\mathrm{nm}). \tag{14}$$

The field dependences of these equations represent a reduction of the Gaussian width due to a stronger overlap of vortices at higher fields, while $\lambda$ is a constant; therefore, the deviation of $\sigma(h)$ from these equations can be attributed to the change of $\lambda$ with the field.

However, the microscopic situation of the FLL state is considerably different from the above 'ideal' one in practical cases where Gaussian damping is actually observed, because there must be an additional effect of randomness to round the sharp feature of $n(B)$. This also makes it difficult to distinguish $\sigma_\mathrm{b}$ from $\sigma$ in equation (11), giving rise to a problem in comparing the values of $\lambda$, for example—between those from an analysis using the modified

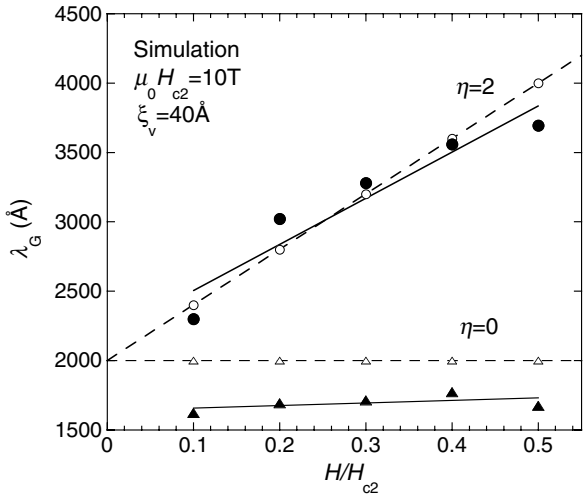


**Figure 2.** The magnetic penetration depth ($\lambda_G$) deduced from an analysis using the Gaussian damping (filled triangles and circles), where the analysed spectra were those simulated by the modified London model with $\overline{\lambda}$ shown by the open triangles (corresponding to $\eta = 0$) and circles ($\eta = 2$) at each field. A linear fit yields $\eta = 0.11$ and 1.53, respectively. The upper critical field was $\mu_0 H_{c2} = 10$ T, from which the cut-off parameter ($\xi_v$) was determined as 40 Å (=$0.7\xi_{GL}$, where $\xi_{GL} = \sqrt{\Phi_0/2\pi H_{c2}}$, with $\Phi_0$ being the quantum flux).

London model and those obtained from the Gaussian approximation (where the influence of $\sigma_b$ is indistinguishable).

In order to examine the model dependence of the analysis, we made a simulation to compare the various results from an analysis where we generated $\mu$SR time spectra using a modified London model and then analysed them by means of simple Gaussian damping (equation (11)) to deduce $\sigma$. According to our result, the Gaussian distribution originates from the distribution of $\lambda$ (which may vary at different sample domains), which must be present in polycrystalline powder specimens of anisotropic superconductors (e.g., $\lambda_c \gg \lambda_{ab}$). As is also clear in the field profile shown in figure 1, the simulated time spectra with typical values for $\lambda$ (2000–3000 Å) cannot be fitted by equation (11) due to the strongly exponential-like damping; this is obviously due to the contribution of high frequency tails in the spectral density, $n(B)$. (Thus, the use of the second moment as an approximation in the ideal situation would be valid only when the relaxation rate is small enough to eliminate the asymmetric feature of $n(B)$.) The situation was much improved when the Gaussian distribution of $\lambda$ was introduced with a variance ($\sigma_\lambda$),

$$G(\lambda) \propto \exp[-(\lambda - \overline{\lambda})^2/\sigma_\lambda^2], \tag{15}$$

where $\overline{\lambda}$ is the mean value. For the parameter values shown in figure 2, the time spectra become Gaussian-like when $\sigma_\lambda \sim$ 600–800 Å, yielding reasonable reduced chi-squared values from equation (11). We also assumed a gradual decrease of $\sigma_\lambda$,

$$\sigma_\lambda(h) = \sigma_\lambda(1 - h^2), \tag{16}$$

considering that the elastic moduli $C_{ii}$ of the FLL, which control the FLL distortion and the associated modulation of $\lambda$, exhibit a quadratic dependence on the applied field. (Note, however, that the factor $1 - h^2$ yields only a small change of $\sigma_\lambda(h)$ for $h < 0.5$.) Some examples are shown in figure 2 for $\sigma_\lambda = 800$ Å, where the penetration depth ($\lambda_G$), obtained using equation (14) from $\sigma(h)$, is plotted together with the original $\overline{\lambda}$. A reasonable agreement between $\lambda_G$ and $\overline{\lambda}$ is seen, except for the case when $\overline{\lambda} = 2000$ Å, where $\lambda_G$ takes systematically lower values at all fields. This can be readily understood by considering the fact that $\sigma$ is enhanced by an amount $\sigma_p$ as a consequence of equation (16). We also examined the field dependence of $\lambda$, which would be most crucial in the following arguments,

$$\lambda(h) = \lambda(0)[1 + \eta h], \tag{17}$$

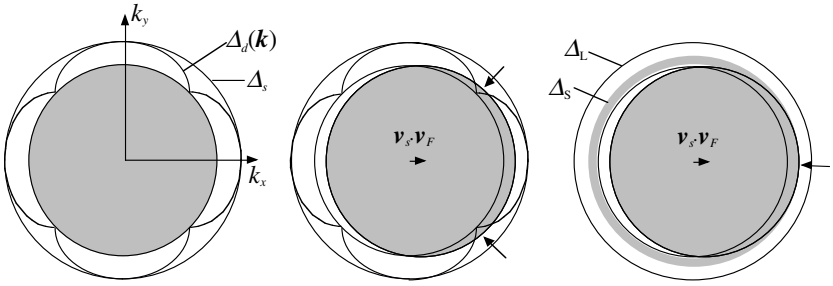


**Figure 3.** The Fermi surface shifted by the quasi-classical Doppler effect due to the supercurrent $\mathbf{v}_s$ around vortices. While such a shift has no effect on the quasiparticle excitation for the isotropic gap ($\varepsilon(\mathbf{v}_F \cdot \mathbf{v}_s) < \Delta_s$), it induces additional excitation by breaking pairs near to the nodal region (centre, pointed by arrows). A similar situation is expected for a multi-gapped order parameter when the sample temperature is greater than that determined by the smallest energy gap ($k_B T \geqslant \Delta_S$).

where $\eta$ is a dimensionless parameter used to express the magnitude of the field dependence. As is evident in figure 2, the slope $d\lambda_G/dh$ is slightly weaker than the original assumption; when we take $\eta = 2$ for the simulation, we obtain $\eta = 1.53$ as the corresponding slope for $\lambda_G$. However, when there is no field dependence of $\overline{\lambda}$ ($\eta = 0$), $\lambda_G$ exhibits the least dependence on the field ($\eta = 0.11$). Thus, we can conclude that the field dependence of the penetration depth (as a mean value) obtained from the Gaussian field approximation provides a sound basis for the characterization of superconductors.

## 3. The Doppler shift and the associated non-linear effect

In the FLL state, the quasiparticle momentum $\mathbf{v}_F$ is shifted by the flow of supercurrent $\mathbf{v}_s$ around the vortices due to a semi-classical Doppler shift, leading to a shift of the quasiparticle energy spectrum by an amount $\varepsilon = m\mathbf{v}_F \cdot \mathbf{v}_s$. Since the density of states (DOS), $N(E)$, is non-zero, except at the Fermi level ($E = 0$) and is higher at larger energy ($0 < E < \Delta_0$) for the anisotropic order parameter, quasiparticles can be excited by the Doppler shift outside of the vortex cores with a population proportional to $N(E+\varepsilon(\mathbf{v}_F \cdot \mathbf{v}_s))$, leading to an enhancement of $\lambda$ [10]. In other words, the Cooper pairs with a gap energy of less than $\varepsilon$ can be broken by the Doppler shift (see figure 3). Historically, a similar effect was considered first for type I superconductors, where the non-linear response of the shielding current in the Meissner effect due to the 'backflow' of quasiparticles was discussed [20].

The magnitude of $\eta$ represents the degree of the increase of the DOS for quasiparticles, which must be roughly proportional to the phase volume of the Fermi surface where the Doppler shift exceeds the gap energy ($\varepsilon(\mathbf{v}_F \cdot \mathbf{v}_s) > \Delta(\mathbf{k})$). It also follows that the effect depends on the direction of $\mathbf{v}_s$ (and hence that of the external field $\mathbf{H}$ relative to the order parameter) in a single-crystalline specimen. According to Volovik, the quasiparticle density of states for the anisotropic order parameter is

$$N_{\mathrm{deloc}}(0) \simeq N_F K \xi_{GL}^2 \sqrt{h} \equiv N_F g(h), \tag{18}$$

$$K \propto \int_{|\Delta(\mathbf{k})|<\varepsilon} |\Delta(\mathbf{k})|\, d\mathbf{k}, \tag{19}$$

where $N_F$ is the DOS for the normal state and $K$ is a constant of the order of unity [10]. As illustrated in figure 3, a similar effect is anticipated for the case of a multi-gapped order parameter; when the sample temperature is greater than that determined by the smallest energy gap ($\sim\Delta_S/k_B$), the corresponding energy band serves effectively as a node in the gap.

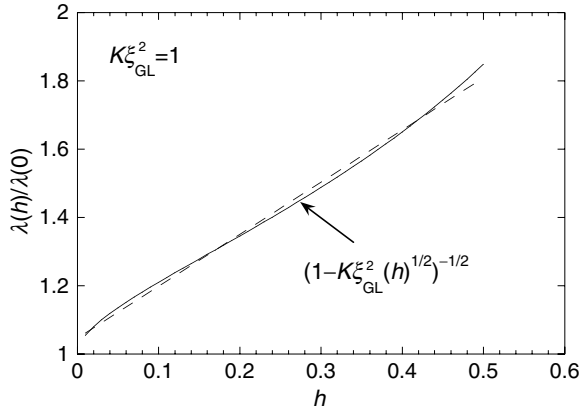


**Figure 4.** The field dependence of λ normalized by the value at $h = 0$ for the case $g(h) = \sqrt{h}$ ($K\xi_{GL}^2 = 1$). It is well represented by a linear dependence, as in equation (22) with $c \sim 1.5$.

It is important to note that $K$ is proportional to the phase volume of the low excitation energy in $\Delta(\mathbf{k})$ (or the relative weight of the band having the smallest energy gap), thereby carrying information on the degree of anisotropy for $\Delta$; the factor $h^{1/2}$ comes from the inter-vortex distance ($\propto h^{-1/2}$) multiplied by the number of vortices ($\propto h$). The superfluid density at a given field is then

$$n_s(h) \simeq n_s(0)[1 - g(h)], \tag{20}$$

which is directly reflected in the magnetic penetration depth,

$$\frac{1}{\lambda^2(h)} = \frac{4\pi e^2}{m^* c^2} n_s(h). \tag{21}$$

Therefore, as a mean approximation, we have

$$\lambda(h) = \frac{\lambda(0)}{\sqrt{1 - g(h)}} \sim \lambda(0)[1 + cK\xi_{GL}^2 h], \tag{22}$$

where $c \simeq 1.5$ for $0 < h < 0.5$, as shown in figure 4. Thus, the comparison between equations (17) and (22) yields

$$\eta \simeq cK\xi_{GL}^2, \tag{23}$$

indicating that the slope $\eta$ reflects the phase volume of the Fermi surface where $|\Delta(\mathbf{k})| < \varepsilon$.

Since the Doppler shift is far smaller than the gap energy in the usual situation for the isotropic gap, no such enhancement is expected for the conventional s-wave pairing ($\eta \ll 1$). A recent theoretical calculation based on the Bogoliubov–de Gennes (BdG) equations indicates, however, that $\eta$ is not exactly zero for s-wave pairing, although it is much smaller than that for $d_{x^2-y^2}$ pairing [21]. It must also be noted that the effect of temperature must be considered to evaluate the degree of anisotropy from the measurement of $\eta$. In general, the phase volume of the Fermi surface where $|\Delta(\mathbf{k})| < k_B T$ also contributes to quasiparticle excitation. Thus, strictly speaking, the observation of a finite $\eta$ means the presence of a small gap region with an upper bound of $\sim k_B T$ (see below: the case of $MgB_2$, for example).

Finally, we point out that the magnitude of $K$ depends on the direction of the Doppler shift relative to the nodes on the Fermi surface. This means that one may be able to determine the angular position of nodes by measuring $\eta$ as a function of the field direction; $\mathbf{v}_s$ is perpendicular to $\mathbf{H}$ and thereby one can control the direction of $\mathbf{v}_s$ via the magnetic field direction. Note, for example, that the situation in figure 3 (centre) corresponds to the case when $\mathbf{H} \parallel k_y$. When we rotate $\mathbf{H}$ by $\psi = \pi/4$ within the $k_x$–$k_y$ plane, the nodes perpendicular to $\mathbf{H}$ do not contribute

to the quasiparticle excitation and thereby $\lambda_c$ must be relatively small for this direction of **H**. Thus, $\lambda_c$ (and thereby $\eta$) is predicted to exhibit an azimuth angle dependence for **H** (no such effect is expected for $\lambda_{ab}$ because $\mathbf{v}_s$ takes all the directions within the $k_x$–$k_y$ plane). While such a possibility is yet to be examined for $\mu$SR, we note that there have been several attempts to measure the azimuth angle dependence of bulk properties including thermal conductivity and electronic specific heat for novel superconductors, for which some interesting results are already reported [22, 23].

## 4. Non-local corrections

Because a superconducting pair correlation occurs over a finite length scale, $\xi_0$ (i.e., the BCS coherence length), the electromagnetic response of superconductors is subject to various non-local effects. The primary example is the cut-off term, $F(K, \xi_v)$, incorporated in the modified London model (equation (4)). Moreover, there are a couple of other corrections that must be considered for anisotropic superconductors.

In the superconducting state with gap nodes in the order parameter, the quasiparticles are mostly confined to the vicinity of the nodes at low temperatures. This generally leads to the suppression of quasiparticle excitation due to the non-local electrodynamics caused by the divergent coherence length, $\xi \propto \Delta(\mathbf{k})^{-1}$, yielding a weaker temperature/field dependence of $\lambda$ at higher fields [24, 25]. Such an effect has been studied experimentally in detail for the case of $YBa_2Cu_3O_{6.95}$ [26, 9].

Another important correction comes from the anisotropy of the Fermi surface. Novel superconductors including cuprates have a common feature that the Fermi surface tends to exhibit a strong anisotropy due to, e.g., a two-dimensional and/or multi-band character, which influences the flow of supercurrent over a length scale $\hbar\mathbf{v}_F/\Delta_0$ [27–30]. More specifically, the length scale is also controlled by the mean free path ($l$) for electrons. It turns out that this non-local correction partially accounts for the change in the vortex lattice structure from triangular to squared lattice in various systems, including $RNi_2B_2C$ (R = Y, Lu) [31–36], $V_3Si$ [37, 38], and $La_{2-x}Sr_xCuO_4$ ($x = 0.17$) [39]. This also leads to a change in $B(\mathbf{r})$ due to the modified flow of supercurrent from a circular to a squared shape (see below; e.g. $YNi_2B_2C$). Note, however, that the difference in free energy between a triangular and a square vortex lattice is fairly small, making the lowest energy configuration strongly dependent on other physical quantities, such as the temperature, magnetic field, and crystal orientation, which is also in a strong correlation with the superconducting order parameter.

## 5. An overview of $\mu$SR results

In this section, we try to establish the correspondence between the presence of the anisotropic order parameter and a non-zero slope ($\eta$) in the magnetic field dependence of $\lambda(h)$. As shown below, $\eta$ provides a good measure for the degree of anisotropy in the superconducting order parameter. However, one has to keep in mind that additional information is generally needed to resolve the precise symmetry of the pairing; one would be easily led to a false conclusion in choosing, e.g., between d- and s + g-wave pairing based solely upon the $\mu$SR result. Another origin of apparent anisotropy would be multi-gap order parameters with one of those having a small gap ($<k_BT$), as suggested in the case of $MgB_2$ (see below).

While a vast body of superconductors have been investigated by means of $\mu$SR, there are not many of them in which the field dependence of $\lambda(h)$ has been measured in detail. This is partly due to the historical reason that the $\mu$SR apparatus with a high magnetic field has become

available for routine service only since the late 1990s. Here, we summarize our recent work on $CeRu_2$, $Y(Pt, Ni)_2B_2C$, $Cd_2Re_2O_7$, and $MgB_2$, for which detailed $\mu$SR measurements have been performed. The results on $NbSe_2$ and $YBa_2Cu_3O_{6.95}$ are also mentioned for a comparison. A wider variety of compounds in relation to other experimental techniques are covered elsewhere [40].

### *5.1. $CeRu_2$*

The cubic Laves phase compound, $CeRu_2$ ($T_c = 6.1$–$6.5$ K at zero field, $\mu_0 H_{c2}(T = 0) \simeq 6$–$7$ T), has a long history of experimental and theoretical studies since its discovery in the 1950s. One of the current issues is its magnetic response at higher fields ($h > 0.5$), where an anomalous enhancement of the quasiparticle excitation has been reported. This is suggested by the observation of de Haas–van Alphen (dHvA) oscillation over a field region where the cyclotron radius is much larger than the inter-vortex distance [41]. The presence of excess quasiparticles has been further confirmed by a strong enhancement of $\lambda$ measured by means of $\mu$SR at higher fields [42]. Moreover, while most of the experimental studies concluded that the pairing symmetry is a spin singlet s-wave, detailed studies on the spin–lattice relaxation in nuclear quadrupole resonance (NQR) suggested the presence of anisotropy in the order parameter [43]. This was apparently in line with the observed non-linear field dependence ($\propto h^{1/2}$) of the electronic specific heat coefficient $\gamma(h)$ [44]; as indicated in equation (18), the quasiparticle excitation has a contribution proportional to $h^{1/2}$ for the anisotropic order parameter, while an $h$-linear dependence is expected for the conventional case, because $\gamma(h)$ must be proportional to the volume of normal cores, and thereby to the number of vortices.

However, our $\mu$SR study on a high quality single crystal has shown that the field dependence of $\gamma(h)$ can be attributed to that of the vortex core radius $\rho_v$ ($\propto \xi_v$), at least over the region $h < 0.5$; the $\mu$SR spectra were analysed (in the frequency domain) using the modified London model to extract $\xi_v$ and $\lambda$ independently [45]. (We later re-analysed some of the data in the time domain and found that the result was unchanged.) When the quasiparticles are confined within the vortex cores, the electronic specific heat coefficient must be proportional to the cross section of the cores multiplied by the number of vortices,

$$\gamma(h) \propto \pi \rho_v^2(h) h = \pi \rho_0^2 h^{\beta}, \tag{24}$$

$$\rho_v(h) = \rho_0 h^{(\beta-1)/2}, \tag{25}$$

where our result for $\rho_v(h)$ is well reproduced by $\beta \simeq 0.53$. It is clear that the observed nearly $h^{1/2}$ dependence of $\gamma(h)$ [44] exhibits perfect agreement with our result. This is also qualitatively in line with a recent theoretical calculation for s-wave superconductors based on the quasi-classical Eilenberger equations, where $\beta \simeq 0.67$ (for $T/T_c = 0.5$) is predicted due to various non-trivial effects, including those from the inter-vortex interaction and the vortex core excitation at finite temperature [46]. This strongly suggests that quasiparticle excitation is confined within the normal cores of the vortices. More importantly, we found that $\lambda(h)$ exhibits the least dependence on $h$ (namely, $\eta \simeq 0$) over the relevant field range, as clearly shown in figure 5 [45]. This is perfectly in line with the above conclusion obtained for the vortex cores, as is also the case with s-wave pairing suggested by the vast majority of other experimental results. Thus, it provides one of the canonical examples for $\lambda(h)$ in the case of isotropic s-wave pairing, as was recently found in $V_3Si$ [47].

Meanwhile, it must be stressed that the situation changes drastically upon increasing the field above $h \sim 0.5$. Figure 5 indicates that $\lambda$ exhibits a divergent increase for $h > 0.6$ with increasing field, thereby suggesting a divergent increase of the quasiparticle excitation. This is strongly supported by the observation of the dHvA effect, as mentioned above. To our

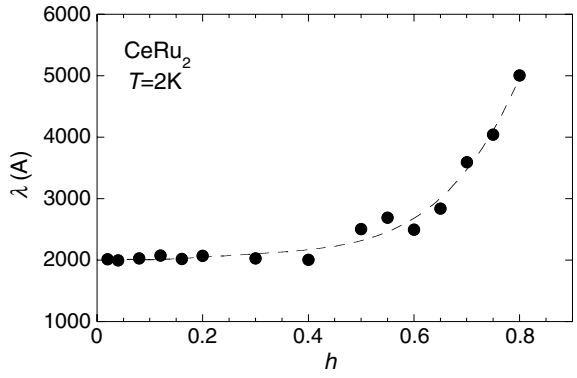


**Figure 5.** The field dependence of the magnetic penetration depth ($\lambda$) in $CeRu_2$ at 2 K obtained by fitting data with the modified London model, where the dashed curve is a guide for the eye (after [45]).

knowledge, there is no simple explanation of such an anomaly[1]. One possible model may be the proposed Fulde–Ferrel–Larkin–Ovchinnikov one, where a new superconducting phase with a spatially inhomogeneous order parameter is predicted to occur in rare-earth compounds having a large spin paramagnetism [49, 50].

Finally, we note that the absence of a clear coherence peak in NQR may be due to the weak random magnetism observed below ∼40 K in zero field $\mu$SR [51]. An increase in the muon spin relaxation rate of the order of 0.02 $\mu s^{-1}$ was observed in accordance with the increase of the ac susceptibility [52]. The sample quality suggests that the weak magnetism is of intrinsic origin, and would act as a scattering source for pair breaking.

### *5.2. Y(Ni, Pt)$_2$B$_2$C*

The borocarbide superconductor, $YNi_2B_2C$ ($T_c = 15.4$ K at zero field, $\mu_0 H_{c2}(T = 0) \simeq 7$–8 T), has attracted much attention due to the strong $h^{1/2}$ dependence of the electronic specific heat coefficient in a high purity specimen [53]. Earlier experiments suggested that an s-wave pairing was realized in this compound because the system showed little sensitivity to non-magnetic impurities, as typically found in BCS s-wave superconductors. As we observed for $CeRu_2$, this led to the speculation of a change of the vortex core radius to reconcile the observed behaviour of $\gamma(h)$ with the presumed isotropic order parameter [53]. It was also found that such an $h^{1/2}$ dependence was replaced by an $h$-linear dependence upon replacement of Ni by Pt ($\simeq$20%). Now, there is mounting evidence that the order parameter in pure $YNi_2B_2C$ is considerably anisotropic [54–57, 23, 58, 59], although the pairing symmetry is basically s-wave-like. The key to understanding the varying results in borocarbides is that the anisotropy of the order parameter is indeed sensitive to impurities, which is in good contrast to the robustness of superconductivity itself; s + g pairing, for example, changes into an effectively isotropic s-wave pairing, where the anisotropic part (associated with the $g$-component) is washed out by impurity scattering. Thus, some of the divided results obtained from NMR $1/T_1$ measurements may be sorted out in terms of the sample purity [40]. Our $\mu$SR study was quite successful in clarifying the effect of non-magnetic impurities on the anisotropic order parameter in $Y(Ni_{1-x}Pt_x)_2B_2C$.

As mentioned before, there is a significant contribution of the non-local effect in borocarbides due to the anisotropy of the Fermi surface. This effect must be considered for

[1] A theoretical calculation by Brandt *et al* [48], which is quoted in [41], points out the possibility that the order parameter is suppressed by an external magnetic field, particularly for the direction of **k** normal to the field. However, the work does not provide a microscopic account of what the origin of the DOS is for the nearly zero-energy excitations that they obtained, despite the situation that the order parameter keeps a finite value outside the vortex cores for $h < 1$.

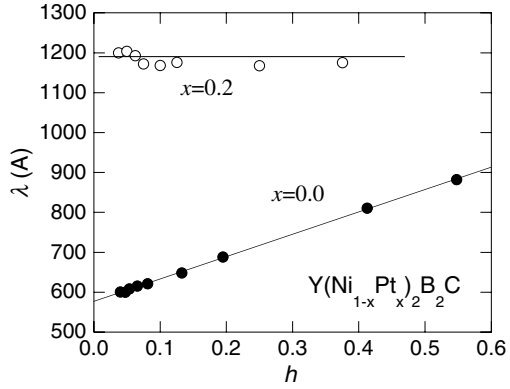


**Figure 6.** The field dependence of the in-plane magnetic penetration depth ($\lambda = \lambda_{ab}$) in $Y(Ni_{1-x}Pt_x)_2B_2C$, obtained by fitting data with the modified London model and a non-local correction, where the data were obtained at 3 K for $x = 0.0$ and 2.5 K for $x = 0.2$ ($T_c = 12.1$ K) (after [36, 60]).

modelling of the magnetic field distribution, $B(\mathbf{r})$, and the associated spectral density, $n(B)$, to obtain the correct values for $\lambda$ and $\xi_v$. To this end, the London model is further modified to yield

$$B(\mathbf{r}) = B_0 \sum_{\mathbf{K}} \frac{e^{-i\mathbf{K}\cdot\mathbf{r}}}{1 + K^2\lambda^2 + (c_1K^4 + c_2K_x^2K_y^2)\lambda^4} F(K, \xi_v), \tag{26}$$

where the terms proportional to $K_x^2K_y^2$ represent the non-local effect, with $c_i$ being the parameters coming from the band structure [28]. Moreover, the non-local effect leads to the formation of a squared flux line lattice, which also modifies $B(\mathbf{r})$. Our result on a single crystal (where $\mathbf{H} \parallel \mathbf{c}$) indicates that these features have a strong influence on $n(B)$ probed by $\mu$SR [36]. For example, no reasonable fit can be obtained when one assumes a square FLL without non-local correction terms.

It has been revealed by our $\mu$SR measurement that the vortex core radius, $\rho_v$, in a pure specimen ($x = 0$) exhibits a much steeper decrease with increasing field than that estimated from the electronic specific heat coefficient, $\gamma(h)$; $\rho_v(h)$ shrinks sharply for $h < 0.1$, then changes only very weakly with the field. This is in marked contrast with the case for $CeRu_2$, where the field dependence of $\gamma(h)$ is in good accord with $\rho_v(h)$ (i.e., $\gamma(h) \propto h\pi\rho_v^2(h)$). This suggests the presence of excess quasiparticle excitation outside of the vortex cores, which contributes to $\gamma$. As shown in figure 6, this is indeed supported by the observation that $\lambda$ exhibits a strong field dependence in a pure specimen. The slope is deduced from the linear fitting (equation (17)) to yield $\eta = 0.95(1)$. On the other hand, for the Pt-doped specimen ($x = 0.2$), $\lambda$ is mostly independent of the field ($\eta \simeq 0$) [60]. This is again consistent with the presumed hybrid nature of the order parameter, where the s-wave component is relatively enhanced by impurity scattering. We also note that $\lambda$ for the Pt-doped specimen is about 1.27 times longer than that expected solely from the conventional impurity effect [60]. This strongly suggests that there is an excess quasiparticle density of states generated by the interaction between the impurities and the anisotropic component of the order parameter, as is found in superconductors with gap nodes.

### *5.3. $MgB_2$*

The revelation of superconductivity in a binary intermetallic compound, $MgB_2$, has attracted much interest because it exhibits an almost two-times-higher transition temperature ($T_c \simeq 39$ K) than those of all intermetallic superconductors known to date [61]. The most interesting issue concerning this compound is whether or not it belongs to the class of the conventional

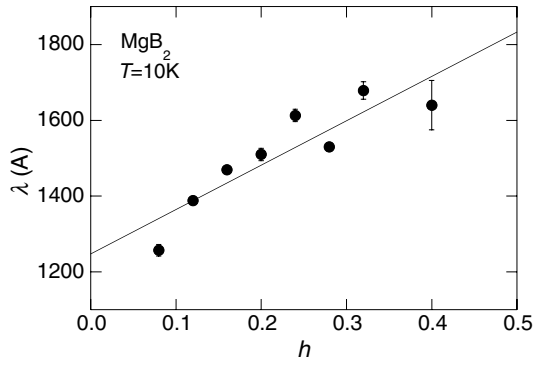


**Figure 7.** The field dependence of the magnetic penetration depth ($\lambda$) in $MgB_2$ obtained by fitting data with the Gaussian field distribution model, where the data were obtained at 10 K. The values for $h < 0.1$ are probably underestimated due to additional relaxation induced by flux pinning (after [79]).

BCS-type (namely, phonon-mediated spin singlet s-wave pairing) superconductors. So far, most experimental results favour phonon-mediated superconductivity [62–69]. On the other hand, calculations of the band structure and the phonon spectrum predict a double energy gap [70, 71], with a larger gap attributed to two-dimensional $p_{x-y}$ orbitals, and a smaller gap to three-dimensional $p_z$ bonding and antibonding orbitals. The experimental results of specific heat measurements [72, 73], point-contact spectroscopy [74], photoemission spectroscopy [75], scanning tunnelling spectroscopy [76] and penetration depth measurements [77] have supported this scenario.

The double energy gap would have a direct relevance for the temperature dependence of $\lambda$, because there must be excess quasiparticles excited over the smaller energy gap ($\Delta_S$) at higher temperatures, while the bulk superconductivity is maintained by the larger gap ($\Delta_L$). At this stage, there are two such $\mu$SR measurements reporting the result of an analysis based on the two-gap model, where $\Delta_S$ is reported to be 2.6(2) meV [78] and 1.2(3) meV [79]. On the other hand, the field dependence of $\lambda$ is sensitive only to those excited by the Doppler shift, and therefore the slope $\eta$ would be zero as long as both energy gaps were isotropic. The only exception would be that the temperature at which $\lambda(h)$ is measured is comparable to $\Delta_S/k_B$, so the smaller gap effectively becomes equivalent to nodes in the order parameter. As shown in figure 7, our result for $\lambda(h)$ exhibits a clear dependence on $h$ with $\eta = 1.27(29)$, where the measurements were performed at $T \simeq 10$ K [79]. Considering that the measured temperature nearly corresponds to $\Delta_S/k_B = 14(4)$ K, the observed field dependence would be qualitatively consistent with the two-gap model with isotropic order parameters. Meanwhile, if the smaller gap is as large as 2.6 meV [78], it would mean that either $\Delta_L$ or $\Delta_S$ is anisotropic.

Unfortunately, so far it is difficult to obtain a single crystal of $MgB_2$ with the dimensions necessary for a conventional $\mu$SR experiment; thus, all of the $\mu$SR measurements have been performed on powder specimens. The time spectra obtained were fitted by the Gaussian field distribution (equation (11)), where the additional relaxation due to the flux pinning ($\propto \exp(-\sigma_p^2 t^2)$) was not separable. As a matter of fact, we observed an *increase* of the relaxation rate with increasing field over the region $h < 0.1$ for our $MgB_2$ specimen, which might be related to the flux pinning [79]. However, as we showed in section 2.2, an analysis based on the Gaussian field distribution model has a relatively weak uncertainty in terms of the *relative* change of $\lambda$ against the field. Thus, we think that the above result provides a sound basis for a qualitative evaluation of the gap anisotropy.

Another source of complication would be that there is a strong anisotropy of magnetic response over the crystal direction, which is mixed up in the polycrystalline specimen; it has been reported that the upper critical field for $H$ parallel to the $ab$-plane ($H_{c2}^{ab}$) is about three times higher than that for the perpendicular direction ($H_{c2}^{c}$) [80]. This introduces an

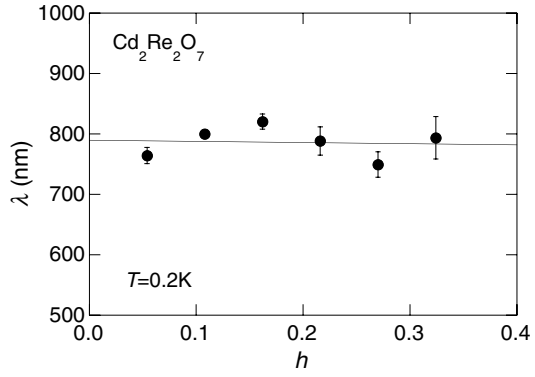


**Figure 8.** The field dependence of the magnetic penetration depth ($\lambda$) in $Cd_2Re_2O_7$ obtained by fitting data with the Gaussian field distribution model, where the data were obtained at 0.2 K (after [91]).

uncertainty in the definition of the normalized field $h$ ($=H/H_{c2}$), which is directly reflected in the evaluation of $\eta$. Thus, further measurements on a single-crystalline specimen would be necessary for the reliable evaluation of $\eta$.

Recently, we made $\mu$SR measurements on a new superconductor, $Ca(Si_{0.5}Al_{0.5})_2$ ($T_c$ = 7.7 K), which has a crystal structure quite similar to that of $MgB_2$ [81]. Provided that the structure of the order parameter in $MgB_2$ is strongly related to that of the Fermi surface, a similar situation might be expected in this compound. Our preliminary result on a polycrystalline specimen with the Gaussian analysis indicates that $\lambda$ exhibits a field dependence with $\eta \simeq 0.8$, thereby supporting the above conjecture, at least in terms of quasiparticle excitation [82].

### 5.4. $Cd_2Re_2O_7$

A class of metal oxides isostructural to the mineral pyrochlore has been attracting considerable attention because they exhibit a wide variety of interesting physical properties [83]. The pyrochlore has a general formula of $A_2B_2O_7$, consisting of $BO_6$ octahedra and eightfold-coordinated A cations, where A and B are transition metals and/or rare-earth elements. In particular, the B sublattice can be viewed as a three-dimensional network of corner-sharing tetrahedra, providing a testing ground for studying the role of geometrical frustration in systems that have local spins at B sites with an antiferromagnetic (AFM) correlation [84]. Although metallic pyrochlores comprise a minority subgroup of the pyrochlore family, they consist of distinct members, such as $Tl_2Mn_2O_7$, which exhibits a colossal magnetoresistance [85, 86]. In view of these backgrounds, the recently revealed superconductivity in 5d transition metal pyrochlores and related oxides, $Cd_2Re_2O_7$ [87, 88] and $KOs_2O_6$ [89], is intriguing, because they evoke anticipation of exotic superconductivity.

It is reported that $Cd_2Re_2O_7$ falls into the bulk superconducting state below $T_c \simeq$ 1–2 K [87]. The dc magnetization curve indicates that the superconductivity is of type II with the upper critical field close to 0.29 T at 0 K. So far, $^{187}$Re NMR $1/T_1$ has exhibited a clear coherence peak typically found for the conventional s-wave pairing [90], although there are not many reports concerned with the pairing symmetry. Thus, the existing evidence strongly suggests that the order parameter is unexpectedly isotropic. This is further supported by the absence of a field dependence for $\lambda(h)$. Figure 8 shows $\lambda(h)$ versus $h$, where one can clearly see that $\eta \simeq 0$ over the observed field range [91]. Here, we note that the upper critical field can be determined by a $\mu$SR measurement when it is well within the reach of the apparatus (<7 T). As is evident in equations (13) and (14), the spin relaxation due to FLL is quenched at $h = 1$ (i.e., $H = H_{c2}$). Thus, from the field dependence of $\sigma$, we obtained $\mu_0 H_{c2} = 0.37(5)$ T

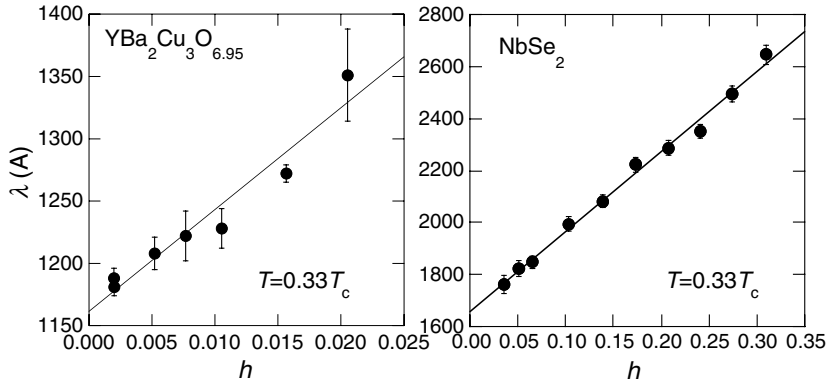


**Figure 9.** The field dependence of the in-plane magnetic penetration depth ($\lambda = \lambda_{ab}$) in $YBa_2Cu_3O_{6.95}$ (YBCO) and $NbSe_2$ at $T = 0.33T_c$, obtained by fitting with the modified London model, where $\mu_0 H_{c2} = 95$ and 2.9 T, respectively. A linear fit yields $\eta = 5$–6.6 for YBCO and 1.85(7) for $NbSe_2$. A slightly smaller value ($\eta = 1.62(6)$) is reported for the latter with an analysis using the GL model (after [9]).

for our specimen. The normalized field in figure 8 is defined by this value for $H_{c2}$. The fact that $\lambda$ exhibits the least dependence on $h$ also means that the field dependence of $\sigma$ is well reproduced by equation (13) or (14) without considering the change in $\lambda$ with the field. A similar field dependence for $\sigma$ is also reported by another group [92].

On the other hand, for $KOs_2O_6$ ($T_c \simeq 9.5$ K), our preliminary $\mu$SR data on a powder specimen exhibit a strong field dependence of $\lambda(h)$ [93], suggesting the presence of anisotropy in the order parameter. This is also consistent with the absence of a coherence peak in the $^{39}$K NMR $T_1$ [94].

### *5.5. Other examples*

As discussed in section 3, quasiparticle excitation due to the Doppler shift is predicted to be stronger for a larger degree of 'manifoldness' in the nodal structure of the order parameter. Thus, it is naturally expected that superconductors with d-wave pairing would exhibit a strong field dependence of $\lambda(h)$. This was proven to be the case by systematic $\mu$SR studies on the vortex state of high $T_c$ cuprates [9]. A typical example is found in $YBa_2Cu_3O_{6.95}$ (see figure 9), in which $\eta$ is reported to be 5–6.6 over a field range $0 < \mu_0 H < 2$ T [95]. The measurement was later extended up to 7 T, where it was found that the field dependence of $\lambda(h)$ became weaker at higher fields ($\eta \sim 2$ for $\mu_0 H > 2$ T) [26]. This is now understood to be a consequence of the non-local correction discussed earlier in section 4. It must be noted that the non-local correction has a strong influence on the temperature dependence of $\lambda$ at higher fields. These results imply that one must be careful about the field range of measurements in evaluating the meaning of $\eta$; the same is true for the slope $\lambda$ against temperature, $d\lambda/dT$.

The last example is $NbSe_2$ [96, 9], where the situation is similar to that for $YNi_2B_2C$ or $MgB_2$. It has been suggested from the non-linear field dependence of $\gamma(h)$ that there must be excess quasiparticles induced by a magnetic field [53]. However, the degree of non-linearity is considerably weaker than that observed in $YNi_2B_2C$, suggesting a smaller anisotropy in the order parameter. This has been supported by other experiments showing that $NbSe_2$ exhibits s-wave pairing with an anisotropic or double-gap structure, where $\Delta_L/\Delta_S \simeq 2$ [97–100]. As shown in figure 9, the absence of nodes, however, does not necessarily mean $\eta = 0$ when the order parameter is anisotropic (or multi-gapped). It happens that a temperature of $\sim 0.33T_c$

**Table 1.** The dimensionless parameter, $\eta$, corresponding to the slope of $\lambda(h)$ against an external field obtained by $\mu$SR. The column 'model' shows the field distribution used for each analysis: 'm-L' for the modified London model, 'GL' for the Ginzburg–Landau model, and 'G' for the Gaussian field distribution. $T$ denotes the temperature where the field dependence of $\lambda$ was measured. The values for $V_3Si$ are based on a preliminary report [47].

| | $T_c$ (K) | Pairing symmetry | $\eta$ | Model | $T$ (K) | $\mu_0 H_{c2}(T)$ (T) |
|---|---|---|---|---|---|---|
| $YNi_2B_2C$ | 15.4 | Anisotropic s (s + g?) | 0.95(1) | m-L | 3.0 | 7.0 |
| $MgB_2$ | 39 | Double gap | 1.3(3) | G | 10.0 | 12.5 |
| $NbSe_2$ | 7.0 | Anisotropic s | 1.85(7) | m-L | 2.3 | 2.9 |
| $YBa_2Cu_3O_{6.95}$ | 93.2 | d | 5–6.6 | m-L | 31.0 | 95 |
| $CeRu_2$ | 6.0 | Isotropic s ($h < 0.5$) | $\simeq$0 | m-L | 2.0 | 5.0 |
| $Y(Ni_{0.8}Pt_{0.2})_2B_2C$ | 12.1 | Isotropic s | $\simeq$0 | m-L | 2.5 | 4.0 |
| $Cd_2Re_2O_7$ | 1–2 | Isotropic s | $\simeq$0 | G | 0.2 | 0.37 |
| $V_3Si$ | 17 | Isotropic s | $\simeq$0 ($h \leqslant 0.25$) | GL | 3.8 | $\sim$16 |

(where measurements were performed) [53, 96] is relatively high, so it is almost comparable to $\Delta_S$. Thus, as discussed earlier, the region around $\Delta_S$ in the Fermi surface works effectively as nodes at such a high temperature.

## 6. Summary and conclusion

We demonstrated that the field dependence of the magnetic penetration depth $\lambda(h)$ provides a sensitive probe for quasiparticles induced by the Doppler shift. As summarized in table 1, the slope $\eta$ is positive when the superconducting order parameter has nodes (or a small gap equivalent to the node at a given temperature), while it is close to zero for the conventional isotropic order parameter. Despite the ambiguity associated with the slight dependence of $\lambda$ on the model employed for the data analysis, the magnitude of $\eta$ provides a good measure of the degree of anisotropy. This would be useful in selecting the pairing symmetry and the associated mechanism of superconductivity for newly discovered materials.

## Acknowledgments

We would like to thank K Machida and M Ichioka for helpful discussion. We are also grateful to J E Sonier for providing the numerical data in figure 9 and for helpful discussion. The $\mu$SR experiment was partially supported by a Grand-in-Aid for Scientific Research on Priority Areas and a Grand-in-Aid for Creative Scientific Research from the Ministry of Education, Culture, Sports, Science and Technology, Japan.

## References

[1] See, for example, *Proc. Int. Conf. on Materials and Mechanisms of Superconductivity High Temperature Superconductors VI (Houston, TX, Feb. 2000)*; *Physica* C **341–348**
[2] Cooper L N 1956 *Phys. Rev.* **104** 1189
[3] Bardeen J, Cooper L N and Schrieffer J R 1957 *Phys. Rev.* **108** 1175
[4] Osheroff D D, Richardson R C and Lee D M 1972 *Phys. Rev. Lett.* **28** 885
[5] Legget A J 1973 *Phys. Rev. Lett.* **31** 352
[6] Anderson P W and Morel P 1961 *Phys. Rev.* **123** 1911
[7] Balian R and Werthamer N R 1963 *Phys. Rev.* **131** 1553
[8] Abrikosov A A 1957 *Sov. Phys.—JETP* **5** 1174
[9] For a recent review, see for example, Sonier J E, Brewer J H and Kiefl R F 2000 *Rev. Mod. Phys.* **72** 769

[10] Volovik G E 1993 *Sov. Phys.—JETP Lett.* **58** 469
[11] Brandt E H 1988 *J. Low Temp. Phys.* **73** 355
[12] Brandt E H 1988 *Phys. Rev.* B **37** 2349
[13] London F and London H 1935 *Proc. R. Soc.* A **149** 71
[14] Yaouanc A, Dalmas de Réotier P and Brandt E H 1997 *Phys. Rev.* B **55** 11107
[15] Brandt E H 1972 *Phys. Status Solidi* b **51** 345
[16] Fesenko V, Gorbunov V, Sidorenko A and Smilga V 1993 *Physica* C **211** 343
[17] Greer A J and Kossler W J 1995 *Low Magnetic Fields in Anisotropic Superconductors* (Berlin: Springer)
[18] Pincus P, Gossard A C, Jaccarino V and Wernick J H 1964 *Phys. Rev. Lett.* **13** 21
[19] Aeppli G, Cava R J, Ansaldo E J, Brewer J H, Kreitzman S R, Luke G M, Noakes D R and Kiefl R F 1987 *Phys. Rev.* B **35** 7129
[20] Bardeen J 1954 *Phys. Rev.* **94** 554
[21] Wang Y and MacDonald A H 1998 *Solid State Commun.* **109** 289
[22] Izawa K, Yamaguchi H, Matsuda Y, Shishido H, Settai R and Onuki Y 2001 *Phys. Rev. Lett.* **87** 057002
[23] Izawa K, Kamata K, Nakajima Y, Matsuda Y, Watanabe T, Nohara M, Takagi H, Thalmeier P and Maki K 2002 *Phys. Rev. Lett.* **89** 137006
[24] Kosztin I and Legget A J 1997 *Phys. Rev. Lett.* **79** 135
[25] Amin M H S, Affleck I and Franz M 1998 *Phys. Rev.* B **58** 5848
[26] Sonier J E, Brewer J H, Kiefl R F, Morris G D, Miller R I, Bonn D A, Chakhalian J, Heffner R H, Hardy W N and Liang R 1999 *Phys. Rev. Lett.* **83** 4156
[27] Affleck I, Franz M and Amin M H S 1997 *Phys. Rev.* B **55** R704
[28] Kogan V G, Bullock M, Harmon B, Miranović P, Dobrosavljević-Gruujić L, Gammel P L and Bishop D J 1997 *Phys. Rev.* B **55** R8693
[29] Kogan V G, Miranović P, Dobrosavljević-Gruujić L, Pickett W E and Christen D K 1997 *Phys. Rev. Lett.* **79** 741
[30] Agterberg D F 1998 *Phys. Rev.* B **58** 14484
[31] Paul D McK, Tomy C V, Aegerter C M, Cubitt R, Lloyd S H, Forgan E M, Lee S L and Yethiraj M 1998 *Phys. Rev. Lett.* **80** 1517
[32] Yethiraj M, Paul D McK, Tomy C V and Thompson J R 1998 *Phys. Rev.* B **58** R14767
[33] Gammel P L, Bishop D J, Eskildsen M R, Mortensen K, Andersen N H, Fisher R I, Cheon K O, Canfield P C and Kogan V G 1999 *Phys. Rev. Lett.* **82** 4082
[34] Sakata H, Oosawa M, Matuba K, Nishida N, Takeya H and Hirata K 2000 *Phys. Rev. Lett.* **84** 1583
[35] Eskildsen M R, Abrahamsen A B, Kogan V G, Gammel P L, Mortensen K, Andersen N H and Canfield P C 2001 *Phys. Rev. Lett.* **86** 5148
[36] Ohishi K *et al* 2002 *Phys. Rev.* B **65** 140505
[37] Yethiraj M, Christen D K, Paul D McK, Miranović P and Thompson J R 1999 *Phys. Rev. Lett.* **82** 5112
[38] Sosolik C E, Stroscio J A, Stiles M D, Hudson E W, Blankenship S R, Fein A P and Celotta R J 2003 *Phys. Rev.* B **68** 140503
[39] Gilardi R *et al* 2002 *Phys. Rev. Lett.* **88** 217003
[40] See, for example, Brandow B H 2003 *Phil. Mag.* **83** 2487
[41] Hedo M, Inada Y, Sakurai K, Yamamoto E, Haga Y and Õnuki Y 1998 *Phil. Mag.* B **77** 975
[42] Yamashita A, Ishii K, Yokoo T, Akimitsu J, Hedo M, Inada Y, Onuki Y, Yamamoto E, Haga Y and Kadono R 1997 *Phys. Rev. Lett.* **79** 3771
[43] Mukuda H, Ishida K, Kitaoka Y and Asayama K 1998 *J. Phys. Soc. Japan* **67** 2101
[44] Hedo M, Inada Y, Yamamoto E, Haga Y, Õnuki Y, Aoki Y, Matsuda T D, Sato H and Takahasi S 1998 *J. Phys. Soc. Japan* **67** 272
[45] Kadono R *et al* 2001 *Phys. Rev.* B **63** 224520
[46] Ichioka M, Hasegwa A and Machida K 1999 *Phys. Rev.* B **59** 184
[47] Sonier J E, Callaghan F D, Miller R I, Noaknin E, Taillefer L, Kiefl R F, Brewer J H, Poon K F and Brewer J D 2004 *Preprint* cond-mat/0401271
[48] Brandt U *et al* 1967 *Z. Phys.* **201** 209
[49] Fulde P and Ferrell R A 1964 *Phys. Rev.* **135** 550
[50] Larkin A I and Ovchinnikov Yu N 1965 *Sov. Phys.—JETP* **20** 762
[51] Huxley A D, Dalmas de Réotier P, Yaouanc A, Caplan D, Couach M, Lejay P, Gubbens P C M and Mulders A M 1996 *Phys. Rev.* B **54** R9666
[52] Nakama T, Hedo M, Maekawa T, Higa M, Resel R, Sugawara H, Settai R, Õnuki Y and Yagasaki K 1995 *J. Phys. Soc. Japan* **64** 1471
[53] Nohara M, Isshiki M, Sakai F and Takagi H 1999 *J. Phys. Soc. Japan* **68** 1078

[54] Terashima T, Haworth C, Takeya H, Uji S, Aoki H and Kadowaki K 1997 *Phys. Rev.* B **56** 5120
[55] Yang I-S, Klein M V, Cooper S L, Canfield P C, Cho B K and Lee S I 2000 *Phys. Rev.* B **62** 1291
[56] Boaknin E, Hill R W, Proust C, Lupien C, Taillefer L and Canfield P C 2001 *Phys. Rev. Lett.* **87** 237001
[57] Izawa K, Shibata A, Matsuda Y, Kato Y, Takeya H, Hirata K, Van Der Beek C J and Konczykowski M 2001 *Phys. Rev. Lett.* **86** 1327
[58] Lipp D, Schneider M, Gladun A, Drechsler S-L, Freudenberger J, Fuchs G, Nenkov K, Mülcher K-H, Cichorek T and Gegenwart P 2002 *Europhys. Lett.* **58** 435
[59] Park T, Salamon M B, Choi E M, Kim H J and Lee S I 2003 *Phys. Rev. Lett.* **90** 177001
[60] Ohishi K *et al* 2003 *Physica* B **326** 364
[61] Nagamatsu J, Nakagawa N, Muranaka T, Zenitani Y and Akimitsu J 2001 *Nature* **410** 63
[62] Bud'ko S L, Lapertot G, Petrovic C, Cunningham C E, Anderson N and Canfield P C 2001 *Phys. Rev. Lett.* **86** 1877
[63] Takahashi T, Sato T, Souma S, Muranaka T and Akimitsu J 2001 *Phys. Rev. Lett.* **86** 4915
[64] Kotegawa H, Ishida K, Kitaoka Y, Muranaka T and Akimitsu J 2001 *Phys. Rev. Lett.* **87** 127001
[65] Chen X K, Konstantinovic M J, Irwin J C, Lawrie D D and Frank J P 2001 *Phys. Rev. Lett.* **87** 157002
[66] Karapetrov G, Iavarone M, Kwok W K, Crabtree G W and Hinks D G 2001 *Phys. Rev. Lett.* **86** 4374
[67] Schmidt H, Zasadzinski J F, Gray K E and Hinks D G 2001 *Phys. Rev.* B **63** 220504
[68] Sharoni A, Felner I and Millo O 2001 *Phys. Rev.* B **63** 220508
[69] Pronin A V, Pimenov A, Loidl A and Krasnosvobodtsev S I 2001 *Phys. Rev. Lett.* **87** 097003
[70] Kortus J, Mazin I I, Belashchenko K D, Antropov V P and Boyer L L 2001 *Phys. Rev. Lett.* **86** 4656
[71] Liu A Y, Mazin I I and Kortus J 2001 *Phys. Rev. Lett.* **87** 087005
[72] Bouquet F, Fisher R A, Phillips N E, Hinks D G and Jorgensen J D 2001 *Phys. Rev. Lett.* **87** 047001
[73] Wang Y, Plackowski T and Junod A 2001 *Physica* C **335** 179
[74] Szabó P, Samuely P, Kamarik J, Klein T, Marcus J, Fruchart D, Miraglia S, Marcenat C and Jansen A G M 2001 *Phys. Rev. Lett.* **87** 137005
[75] Tsuda S, Tokoya T, Kiss T, Takano Y, Togano K, Kitou H, Ihara H and Shin S 2001 *Phys. Rev. Lett.* **87** 177006
[76] Giubileo F, Roditchev D, Sacks W, Lamy R, Thanh D X and Klein J 2001 *Phys. Rev. Lett.* **87** 177008
[77] Manzano F, Carrington A, Hussey N E, Lee S, Yamamoto A and Tajima S 2002 *Phys. Rev. Lett.* **88** 047002
[78] Niedermayer Ch, Bernhard C, Holden T, Kremer R K and Ahn K 2002 *Phys. Rev.* B **65** 094512
[79] Ohishi K, Muranaka T, Akimitsu J, Koda A, Higemoto W and Kadono R 2003 *J. Phys. Soc. Japan* **72** 29
[80] Shi Z X, Tokunaga M, Tamegai T, Takano Y, Togano K, Kito H and Ihara H 2003 *Phys. Rev.* B **68** 104513
[81] Imai M, Nishida K, Kimura T and Abe H 2002 *Appl. Phys. Lett.* **80** 1019
[82] Kuroiwa S, Takagiwa H, Yamazawa M, Akimitsu J, Ohishi K, Koda A, Higemoto W and Kadono R 2004 *Preprint* cond-mat/0402483
[83] Subramanian M A, Aravamudan G and Rao V G S 1983 *Prog. Solid State Chem.* **15** 55
[84] Ramirez A P 1994 *Annu. Rev. Mater. Sci.* **24** 453
[85] Shimakawa Y, Kubo Y and Manako T 1996 *Nature* **379** 53
[86] Shimakawa Y, Kubo Y, Manako T, Sushko Y V, Argyriou D N and Jorgensen J D 1999 *Phys. Rev.* B **55** 6399
[87] Hanawa M, Muraoka Y, Tayama T, Sakakibara T, Yamaura J and Hiroi Z 2001 *Phys. Rev. Lett.* **87** 187001
[88] Jin R, He J, McCall S, Alexander C S, Drymiotis F and Mandrus D 2001 *Phys. Rev.* B **64** 180503
[89] Yonezawa S, Muraoka Y, Matsushita Y and Hiroi Z 2004 *J. Phys.: Condens. Matter* **16** L9
[90] Vyaselev O, Arai K, Kobayashi K, Yamazaki J, Kodama K, Takigawa K, Hanawa M and Hiroi Z 2002 *Phys. Rev. Lett.* **89** 017001
[91] Kadono R, Higemoto W, Koda A, Kawasaki Y, Hanawa M and Hiroi Z 2002 *J. Phys. Soc. Japan* **71** 709
[92] Lumsden M D, Dunsiger S R, Sonier J E, Miller R I, Kiefl R F, Jin R, He J, Mandrus D, Bramwell S T and Gardner J S 2002 *Phys. Rev. Lett.* **89** 147002
[93] Koda A, Higemoto W, Ohishi K, Saha S R, Kadono R, Yonezawa S, Muraoka Y and Hiroi Z 2004 *Preprint* cond-mat/0402400
[94] Takigawa M 2004 private communication
[95] Sonier J E *et al* 1997 *Phys. Rev.* B **55** 11789
[96] Sonier J E, Kiefl R F, Brewer J H, Chakhalian J, Dunsiger S R, MacFarlane W A, Miller R I, Wong A, Luke G M and Brill J W 1997 *Phys. Rev. Lett.* **79** 1742
[97] Hess H F, Robinson R B and Waszczak J V 1990 *Phys. Rev. Lett.* **64** 2711
[98] Sanchez D, Junod A, Muller J, Berger H and Lévy F 1995 *Physica* B **204** 167
[99] Ishida K, Nino Y, Zheng G-Q, Kitaoka Y, Asayama K and Ohtani T 1996 *J. Phys. Soc. Japan* **65** 2341
[100] Boaknin E *et al* 2003 *Phys. Rev. Lett.* **90** 117003